Nucleotide Release and Associated Conformational Changes Regulate Function in the COOH-Terminal Src Kinase, Csk†

Jennifer Shaffer,‡ Gongqin Sun,§ and Joseph A. Adams*,‡

Department of Pharmacology, University of California, San Diego, La Jolla, California 92093-0506, and Department of Cell and Molecular Biology, University of Rhode Island, Kingston, Rhode Island 02881

Received May 21, 2001; Revised Manuscript Received July 19, 2001

ABSTRACT: The COOH-terminal Src kinase (Csk) regulates a broad array of cellular processes via the specific phosphorylation and downregulation of Src family protein kinases. While Csk has been a topic for steady-state kinetic studies, the individual steps associated with substrate phosphorylation have not been investigated. To understand active-site phenomena, pre-steady-state and transient-state kinetic methods were applied to develop a catalytic pathway for substrate processing. Rapid quench flow techniques show that the phosphorylation of a substrate peptide, generated from a random library, occurs in two kinetic phases: a rapid, exponential "burst" phase followed by a slow, linear phase. The amplitude of the burst phase increases as a function of enzyme concentration, indicating that the biphasic kinetics are not the result of product inhibition. Analysis of the burst rate as a function of substrate concentration indicates that the phosphoryl transfer step is fast ($k_3 \geq 140\ s^{-1}$) and highly favorable ($k_3/k_{-3} \geq 6$). The apparent dissociation rate constant for ADP ($0.6\ s^{-1}$), measured using stopped-flow kinetic methods and a fluorescent trapping agent, mant-ATP, is close to k_{cat}. Since the substrate dissociation constant is high, the release of phosphopeptide is not likely to limit turnover. These findings indicate that Csk rapidly delivers the γ-phosphate of ATP to the substrate and rapidly releases the phosphoproduct. Overall rate limitation in the steady state is then attributed to the slow, net dissociation of ADP. Viscosometric studies suggest that this final event in the catalytic cycle is coupled with slow conformational changes.

Protein kinases are the essential catalysts that facilitate protein phosphorylation, an essential posttranslational modification that has broad effects on many cellular events. While normally under stringent control, protein kinases that have escaped their regulatory confines through genetic alterations have been linked to disease (*2*). Accordingly, the protein kinases are highly relevant drug targets, and a number of kinase-directed agents are currently in clinical phase trials (*3*). Given the importance of this enzyme family and their inherent complexity, protein kinases are under fierce investigation. It has become apparent in recent years that understanding function is best derived in an appropriate setting where individual steps associated with catalysis can be clearly identified and evaluated (*1*, *4*−*13*). The introduction of fast mixing kinetic methods, initially pioneered on the paradigm protein kinase, PKA[1] (*1*, *14*), has presented a sophisticated view of catalysis. These approaches have provided an excellent backdrop for studying the ATP and substrate binding pockets in PKA (*7*, *15*, *16*).

In PKA, many of the steps associated with substrate processing, including the phosphoryl transfer step, are fast (*1*). At high concentrations of Mg^{2+}, the rate-limiting step in turnover is ADP release (*14*). Under physiological concentrations of this metal, product release (ADP) is only partially rate-limiting, implying that slow conformational changes are important for turnover (*17*). The role of conformational changes in protein kinases may not be a unique phenomenon isolated to PKA. Recent kinetic studies on HER-2, the human epidermal growth factor receptor, show that this protein tyrosine kinase (PTK) rapidly binds and phosphorylates substrates (*12*). On the basis of transient-state kinetic investigations, turnover was shown to be limited partly by ADP release and a slow conformational change (*12*). Hydrogen−deuterium exchange studies indicate that nucleotide binding to PKA induces long-range structural changes that involve domain and secondary structure motions (*18*). Such solution studies may provide a potential link between slow conformational change steps detected in the kinetic studies (*17*, *19*) and the static X-ray models (*20*). Whether ADP release and/or slow structural changes will limit substrate phosphorylation in other members of the protein kinase family is presently unknown. While the predicted number of protein kinases encoded by the vertebrate genome is large (*21*), fast mixing kinetic studies, which can uniquely provide information about conformational changes, are available for only two members of the family, to date (*1*, *12*). The absence of more transient-state kinetic analyses is rooted partly in difficulties in expressing large quantities of pure and active kinases.

† This work was supported by NIH Grant CA 75112 and a BioSTAR award (B99-52).

* To whom correspondence should be addressed. Telephone: (858) 822-3360. Fax: (858) 822-3361. E-mail: joeadams@ucsd.edu.

‡ University of California, San Diego.

§ University of Rhode Island.

[1] Abbreviations: Csk, COOH-terminal Src kinase; GST, glutathione *S*-transferase; GST−Csk, fusion protein of GST and Csk; HER-2, human epidermal growth factor receptor PTK; InRK, kinase domain of the insulin receptor; mant-ATP, 2′(3′)-*O*-(*N*-methylanthraniloyl)-adenosine 5′-triphosphate; nrPTK, nonreceptor PTK; PKA, cAMP-dependent protein kinase; PTK, protein tyrosine kinase.

10.1021/bi011029y CCC: $20.00
Published on Web 08/24/2001

Csk plays a pivotal role in downregulating all members of the Src family of nonreceptor PTKs (nrPTKs) through the C-terminus (*22*, *23*). Through its inactivation of this enzyme family, Csk has profound effects on T cell regulation, cystoskeletal organization, and neural development (*22*, *24*, *25*). Csk is composed of three key structural domains: SH2, SH3, and kinase domains. While only the X-ray structure for the kinase domain of Csk is available (*26*), the full-length enzyme is likely to resemble the three-dimensional structure for c-Src (*27*−*29*). However, unlike those of Src family nrPTKs, the activity of Csk is not modulated through phosphorylation (*26*). Csk has been extensively studied using traditional steady-state kinetic methods and a range of substrates, including Src proteins, short peptides, and heteropolymers (*30*−*36*). Employing viscosometric methods to investigate the rate-limiting steps in Csk, Cole and colleagues concluded that phosphoryl transfer and ADP release are partially rate-limiting for turnover (*30*, *31*). We have shown in previous studies on PKA that viscosity effects can be detected on slow conformational change steps, making the assignments of unimolecular and bimolecular steps troublesome (*17*, *19*). To circumvent these difficulties, we employed pre-steady-state and transient-state kinetic methods to Csk to assess the individual steps in the catalytic pathway. We found that the rates of substrate binding, phosphoryl transfer, and phosphoproduct release are fast while ADP release and associated conformational changes fully limit turnover.

EXPERIMENTAL PROCEDURES

Materials. Dithiothreitol (DTT), ethylenediaminetetraacetic acid, disodium salt dihydrate (EDTA), glycerol, isopropyl β-thiogalactoside (IPTG), β-mercaptoethanol (BME), methylisatoic anhydride, sucrose, and tris(hydroxymethyl)aminomethane (Tris) were purchased from Fisher. Adenosine 5′-triphosphate (ATP), glutathione−agarose beads, and thrombin were obtained from Sigma. [γ-^{32}P]ATP was purchased from NEN. Cellulose resin DE52 was purchased from Whatman. Media supplies (bacto-agar, yeast extract, and tryptone peptone) were purchased from Difco.

Proteins, Peptides, and Fluorescent Nucleotide Derivatives. The fusion protein, GST−Csk, was expressed and purified according to previously published procedures using glutathione−agarose beads (*37*). The fusion protein was cleaved by mixing GST−Csk (3 mg/mL) and thrombin (100 units/mg of GST−Csk) in 50 mM Tris (pH 7.5), 150 mM NaCl, 2.5 mM $CaCl_2$, and 10% glycerol and incubating for 30 min at 4 °C (*38*, *39*). Csk was separated from GST and uncleaved fusion protein using a Q-Sepharose column (Pharmacia) with a 50 to 300 mM NaCl gradient [20 mM phosphate buffer (pH 7.5)]. GST−Csk and Csk were stored at −80 °C in 50 mM Tris (pH 7.5) and 10% glycerol in small aliquots. The substrate peptide, $K_4E_2IYF_3$, was synthesized at the University of Southern California Microchemical Core Facility (Los Angeles, CA) using Fmoc chemistry, and purified by C-18 reverse-phase HPLC. The peptide was resuspended in 50 mM Tris (pH 7.5), and the concentration was determined by weight. Mant-ATP was synthesized using methylisatoic anhydride and purified using ion exchange chromatography according to a previously published procedure (*40*).

Radiochemical Assay. Csk was assayed using a radiochemical assay. Typically, Csk is preequilibrated with [γ-^{32}P]-ATP (0.4 mM, 600−2000 cpm/pmol) prior to mixing with substrate peptide in the presence of $MnCl_2$ in 50 mM Tris (pH 7.5), 0.1% Triton, and 5 mM BME at 30 °C. In all experiments, the free concentration of Mn^{2+} is held constant at 5 mM using a stability constant of 10 μM (*41*). The reaction is terminated using 30% acetic acid. The phosphorylated peptide is separated from unreacted, labeled ATP using a DE52 column (1 mL of resin) preequilibrated with 30% acetic acid (*9*). The total counts per minute of the eluted material is then determined using a scintillation counter. Control reactions are performed in which Csk is added to an acid-quenched mixture of [γ-^{32}P]ATP and substrate peptide, and the counts per minute are subtracted from the reaction samples.

Rapid Quench Flow Methods. The phosphorylation of the substrate peptide by Csk was monitored using a KenTech rapid quench flow instrument (RQF3) and a previously published procedure (*1*). In one reaction loop, Csk (5−10 μM) is preequilibrated with [γ-^{32}P]ATP (0.4 mM, 1000−3000 cpm/pmol) and 5 mM free Mn^{2+}. The reactions are initiated by mixing with an equal volume of substrate peptide (1−5 mM) containing $MnCl_2$. The reactions are performed in 50 mM Tris (pH 7.5), 0.1% Triton, and 5 mM BME at 30 °C. In all experiments, the free concentration of Mn^{2+} is held constant at 5 mM. The reaction is quenched with 30% acetic acid, and the sample is analyzed using the radiochemical assay. Control experiments are performed in which acetic acid is included with the substrate peptide in one of the sample loops. The counts from these control experiments are subtracted from the reaction counts per minute. The specific activity of the [γ-^{32}P]ATP is determined by performing complete turnover experiments using limiting amounts of ATP and excess substrate peptide.

Stopped-Flow Fluorescence Methods. The binding of mant-ATP to Csk was monitored using an Applied Photophysics stopped-flow spectrophotometer (SX-18MV). Samples were mixed in equal volumes, and fluorescence changes were detected using an excitation wavelength of 340 nm and a 420 nm cutoff filter. A total of 400 points were taken for each trace, and between 5 and 15 traces were averaged. The fluorescence output was recorded in volts. All experiments were performed in 50 mM Tris (pH 7.5) and 0.1% Triton at 30 °C using 5 mM free Mn^{2+}.

Data Analysis. The counts per minute from the rapid quench flow experiments corrected for background were converted to concentrations of phosphopeptide using the specific activity of ATP. The time-dependent production of phosphopeptide is fit to eq 1

$$[P] = \alpha[1 - \exp(-k_b t)] + L_t \quad (1)$$

where α, k_b, and L are the burst phase amplitude, the burst phase rate, and the linear phase rate, respectively. The initial velocity data were fit to the Michaelis−Menten equation to obtain K_m and V_{max}. The V_{max} values were converted to k_{cat} using the total enzyme concentration determined from a Bradford assay ($k_{cat} = V_{max}/E_{tot}$).

RESULTS

Purification and Structural Characterization of Csk. GST−Csk is readily purified in milligram quantities by

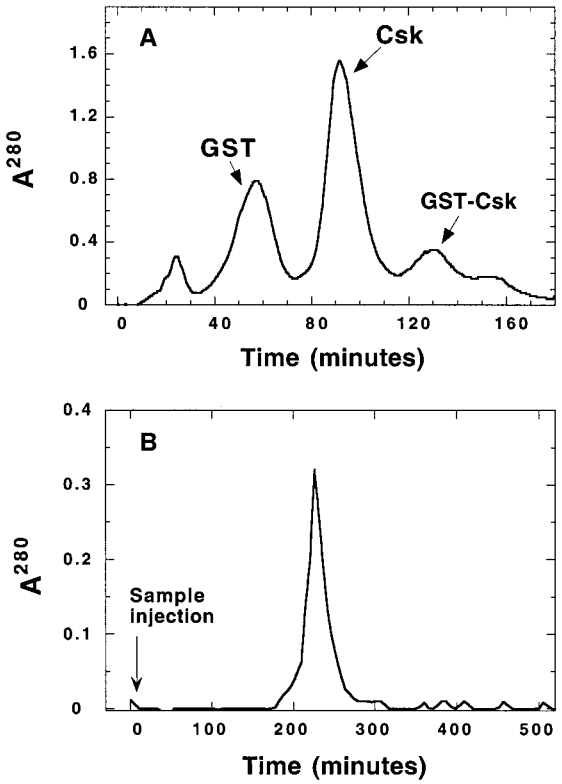

FIGURE 1: Purification of Csk using ion exchange and size exclusion chromatographies. (A) Separation of Csk from GST and uncleaved fusion protein, GST−Csk, using a Q-Sepharose column. GST−Csk (purified on g-agarose) is cleaved with thrombin, bound to the column, and then eluted with a gradient of 50 to 300 mM NaCl in 20 mM phosphate buffer (pH 7.5). The identification of the individual peaks was carried out using a polyacrylamide gel. (B) Elution of Csk on a size exclusion column. Purified Csk is run through an S100 size exclusion column in 20 mM phosphate buffer and 5 mM BME (pH 7.5). The proteins were detected using absorbance readings at 280 nm (A_{280}).

affinity chromatography using a glutathione−agarose resin (*37*). In addition to the incorporation of the GST fusion partner, the plasmid from which Csk is derived contains a streptavidin (strep) tag on the C-terminus (*37*). The introduction of the latter reduces the extent of cellular proteolysis and further assists in purification. While GST or the strep tag provides complementary means for quickly separating cleaved Csk from GST, we elected to purify Csk from free GST and GST−Csk using ion exchange chromatography (Figure 1). The application of bacterial expression systems to protein kinases can be sometimes problematic due to the production of insoluble or inactive protein. Because of the latter dilemma, the use of separation techniques that rely upon the biophysical parameters of Csk rather than the affinity tags allows a thorough physical characterization of the target enzyme during purification. As shown in Figure 1A, Csk elutes as a single peak from an ion exchange column (Q-Sepharose) and can be separated from uncleaved GST−Csk and GST. When applied to a size exclusion column (S100), purified Csk elutes as a single, symmetric peak with no high-molecular weight aggregates found in the flowthrough (Figure 1B). Standardization of the column with known protein samples provides an apparent M_r of 51 000 for Csk, in keeping with the expected molecular weight. Thus, Csk is purified as a folded, monomeric protein from the bacterial host.

Steady-State Kinetic Studies. For the kinetic studies, we employed a short substrate peptide ($K_4E_2IYF_3$) derived from a random library search (*33*). This peptide has been reported to display poor solubility in the kinase reaction (*33*). While we have found that this peptide is very soluble in stock solutions, it precipitates at >0.5 mM in the presence of low ATP concentrations (0.2 mM) in our hands. To circumvent this problem, 0.1% Triton was included in the activity assays. This nonionic detergent permits concentrations of 5−10 mM substrate peptide to be achieved with no sign of precipitation in the presence of 1 mM ATP. With conditions optimized, we measured the steady-state kinetic properties for the phosphorylation of this substrate using the radiochemical assay. The initial velocity of the reaction was monitored as a function of substrate peptide (0.1−10 mM) at fixed concentrations of ATP (1 mM) and Csk (3 μM). From this plot, the K_m and k_{cat} are 5 ± 2 mM and 0.12 ± 0.03 s^{-1}, respectively. A prior K_m measurement for this peptide is lower at 0.5 mM (*33*). The discrepancies between this report and those presented here may be related to the incorporation of Triton in our assay mixtures. We have attempted to measure the K_m for the peptide in the absence of Triton but observed obvious precipitation problems at >0.5 mM (data not shown). Despite the differences in the apparent substrate peptide affinity, the K_m for ATP is very similar to previous reports indicating that the difference in apparent substrate peptide affinity is not due to variations in the protein sample preparation (*30*−*32*). At 5 mM substrate peptide, the K_m for ATP was found to be 20 μM.

Viscosity Effects on the Steady-State Kinetic Parameters. The influence of viscosogens on k_{cat} has been analyzed extensively for Csk using $polyGlu_4Tyr$ as a substrate in the presence of Mn^{2+} (*30*). Increasing solvent viscosity reduces this parameter to an intermediate level that is consistent with a kinetic mechanism where phosphoryl transfer is partially rate-limiting (*30*). Using $K_4E_2IYF_3$ as a substrate, the steady-state kinetic parameters for Csk were measured in the absence and presence of 25% sucrose to determine the effects of viscous media on phosphorylation. In this experiment, Csk (3 μM), preequilibrated with [γ-^{32}P]ATP (1 mM), is mixed manually with substrate peptide (0.5−10 mM) in 50 mM Tris (pH 7.5), 0.1% Triton, and 5 mM BME containing 0 or 25% sucrose. The initial velocity of the reaction is plotted as a function of substrate peptide concentration to determine the kinetic parameters. The values for k_{cat} and k_{cat}/K_m are 0.15 ± 0.01 s^{-1} and 0.03 ± 0.004 mM^{-1} s^{-1} at 0% sucrose and 0.20 ± 0.01 s^{-1} and 0.10 ± 0.02 mM^{-1} s^{-1} at 25% sucrose, respectively. Thus, increasing the relative solvent viscosity by a factor of 2 [$\eta^{rel} = 2.1$ at 25% sucrose (*30*)] causes a modest increase in k_{cat} (33%) and a significant increase in k_{cat}/K_m (300%) with the substrate peptide. The latter effect results from large decreases in the K_m for the substrate peptide at high sucrose concentrations. A similar effect has been reported previously for Csk and $polyGlu_4Tyr$ as a substrate (*30*), but the source of this phenomenon is not fully understood.

Rapid Quench Flow Kinetic Studies. The phosphorylation of the substrate peptide, $K_4E_2IYF_3$, was monitored as a function of time using a rapid quench flow instrument. The time-dependent production of phosphopeptide is shown in Figure 2A in the presence of 5 mM substrate peptide, 0.4

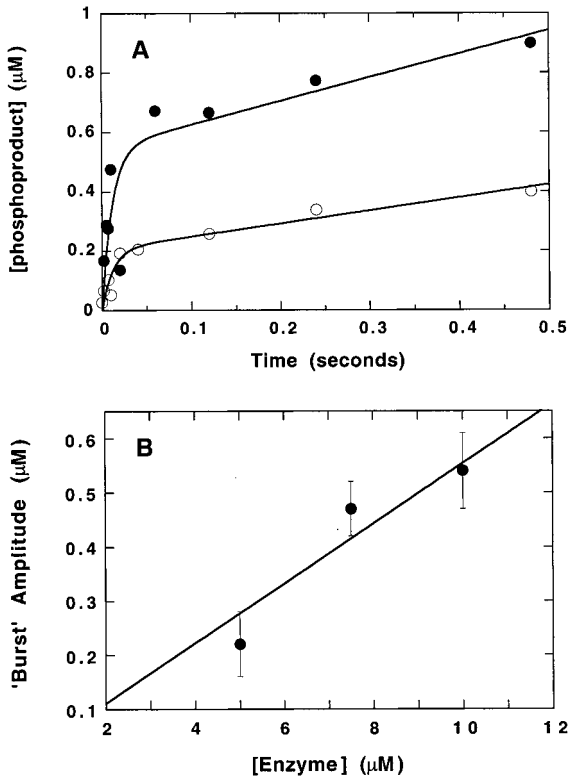

FIGURE 2: Pre-steady-state kinetic traces for the Csk-catalyzed phosphorylation of the substrate peptide, $K_4E_2IYF_3$. (A) Effects of Csk concentration on the kinetic transients. [γ-^{32}P]ATP (0.40 mM) is preequilibrated with 5 (○) and 10 μM Csk (●), and the reaction is initiated with 5 mM substrate peptide in the rapid quench flow instrument. The data are fit to eq 1, and the parameter fits are given in Table 1. (B) Effects of Csk concentration on the burst amplitude. The data from Table 1 are plotted and fitted with a linear function where the slope is 0.06.

Table 1: Pre-Steady-State Kinetic Parameters at Varying Substrate Peptide and Csk Concentrations[a]

E_{tot} (μM)	[S] (mM)	α (μM)	k_b (s^{-1})	L (μM/s)	L/E_{tot} (s^{-1})	α/E_{tot}
10	5	0.54 ± 0.07	85 ± 12	0.80 ± 0.29	0.080	0.054
5	5	0.21 ± 0.02	85 ± 15	0.42 ± 0.08	0.084	0.040
7.5	5	0.47 ± 0.05	95 ± 15	0.60 ± 0.12	0.080	0.063
7.5	2.5	0.30 ± 0.03	62 ± 9	0.36 ± 0.08	0.045	0.040
7.5	1	0.10 ± 0.02	34 ± 10	0.18 ± 0.06	0.024	0.013

[a] These parameters are derived from fitting the data in Figures 2 and 3 to eq 1.

mM ATP, and two concentrations of Csk (5 and 10 μM). At both enzyme concentrations, the data are ostensibly biphasic with a rapid, exponential rise in the amount of phosphopeptide (burst phase) followed by a slow, linear phase. The data were fit to eq 1, and the individual parameter outputs are listed in Table 1. A pre-steady-state kinetic transient was also collected at 7.5 μM Csk (data not shown), and the parameter fits are displayed in Table 1. The enzyme-normalized linear rates (L/E_{tot}), in all cases, are consistent with the steady-state kinetic rates measured in typical, manual mixing assays, indicating that the linear phase in the rapid quench flow experiments appropriately reflects the steady-state phase. The observed burst amplitudes at all three Csk concentrations are shown plotted in Figure 2B. The data were fit to a line function with a slope of 0.06. This slope indicates that the burst amplitude (α) reflects 6% of the total protein

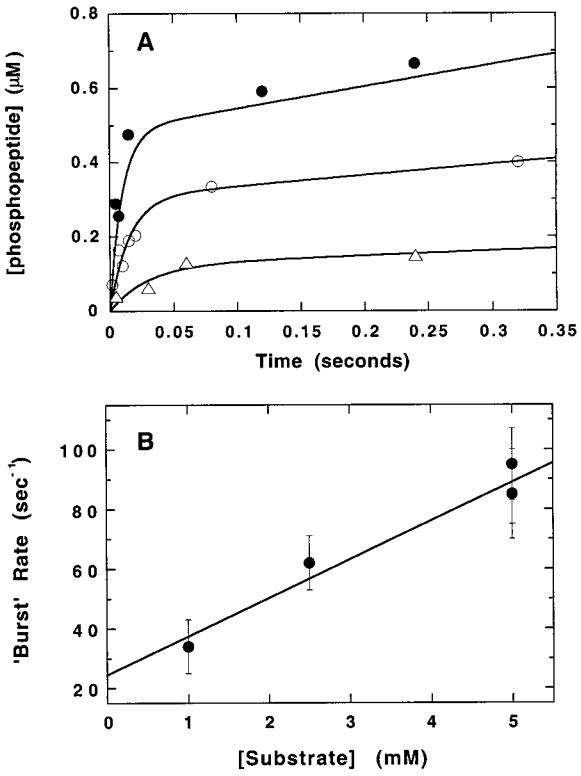

FIGURE 3: Effects of substrate peptide concentration of the pre-steady-state kinetic transients for Csk. (A) Kinetic transients at three different substrate peptide concentrations. Csk (7.5 μM) is pre-equilibrated with ATP (0.4 mM) and mixed with 1 (△), 2.5 (○), and 5 mM substrate peptide (●). The data are fit to eq 1, and the parameter fits are included in Table 1. Only the first 350 ms is shown for clarity. (B) Substrate dependence on the observed burst phase rate. The data are fit to a line function to obtain a slope of 13 ± 2 mM^{-1} s^{-1} and an intercept of 25 ± 6 s^{-1}.

concentration based on a Bradford assay at 5 mM substrate peptide.

Effects of Substrate Peptide Concentration on Pre-Steady-State Kinetics. To further characterize Csk, the pre-steady-state kinetics were monitored as a function of substrate peptide concentration at fixed enzyme concentration. In the rapid quench flow instrument, Csk (7.5 μM) was preequilibrated with ATP (0.4 mM) and mixed with 1, 2.5, and 5 mM substrate peptide. Time points ranging from 2 ms to 1 s were analyzed. The production of phosphopeptide in the first 350 ms is shown in Figure 3A. The data were fit to eq 1, and the parameter outputs are included in Table 1. Both the burst amplitudes and linear rates increase as a function of substrate peptide concentration. The latter values directly parallel the expected changes in L as a function of substrate peptide concentration. For example, the expected values for L/E_{tot} from the Michaelis−Menten equation are 0.06, 0.04, and 0.02 s^{-1} at 5, 2.5, and 1 mM substrate peptide, respectively, and are close to the experimental values in Table 1. The burst rate constant increases linearly as a function of substrate concentration with a slope of 13 ± 2 mM^{-1} s^{-1} and a ***y***-intercept of 25 ± 6 s^{-1} (Figure 3B).

Stopped-Flow Fluorescence Experiments. In previous studies, it was shown that the kinetic binding of mant nucleotide derivatives to PKA and HER-2 could be monitored using stopped-flow fluorescence spectroscopy (*12*, *40*). To determine the dissociation rate constant for dissociation of ADP from Csk, we utilized one of these derivatives, mant-

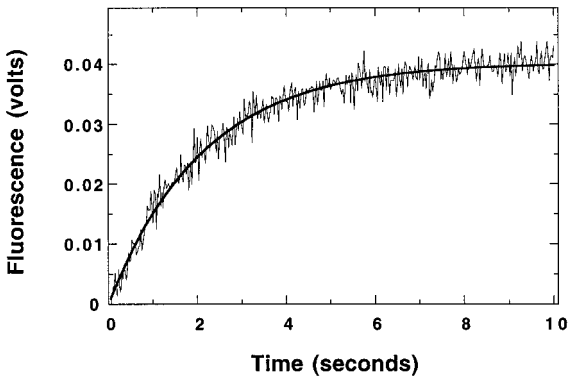

FIGURE 4: Displacement of Csk-bound ADP using mant-ATP as a trapping agent in the stopped-flow instrument. The initial concentrations of Csk, ADP, and mant-ATP are 2, 100, and 600 μM, respectively. The data are fit to single-exponential functions to provide a rate constant of 0.60 $\pm$ 0.05 s^{-1}.

ATP, as a trapping agent. In these experiments, Csk (2 μM) is preequilibrated with ADP (100−200 μM) in one syringe and then rapidly mixed with high concentrations of mant-ATP (600−1200 μM) in the second syringe. On the basis of prior K_I measurements, this level of ADP saturates all the binding sites (*6*). Changes in mant fluorescence were monitored above 420 nm using an excitation wavelength of 340 nm. A typical kinetic transient is shown in Figure 4. Dissociation of ADP is monitored by a time-dependent increase in fluorescence as mant-ATP binds to the free enzyme resulting from decomposition of the binary enzyme−ADP complex. The data are fit to a single-exponential function to produce a rate constant of 0.60 $\pm$ 0.10 s^{-1}. Doubling the concentration of mant-ATP (1200 μM) did not alter the rate of the transient, indicating that the experiments are performed under adequate trapping concentrations (data not shown). Also, doubling the ADP concentration (200 μM) at 1200 μM mant-ATP had no effect on the fitted rate constant, indicating that the observed fluorescence increase is not due to the trapping agent binding free Csk present in the initial enzyme−ADP mixture. Control experiments were performed to determine a minimal rate at which mant-ATP binds to Csk in the absence of ADP. In this experiment, Csk (1 μM) is mixed with mant-ATP (40 μM) in the stopped-flow instrument. A rise in fluorescence that exceeded 200 s^{-1} was observed in the presence of either metal (data not shown). This observed binding rate is similar to that observed for mant-ATP binding to PKA (*40*). Since this binding rate for Csk is much faster than the observed trapping rate for ADP, the observed transients are not limited by binding of the fluorophore.

DISCUSSION

As a key regulator of Src-related enzymes, Csk has been extensively studied using steady-state kinetic methods (*6*, *30*−*32*, *34*, *35*). While important for a complete functional understanding, the steady-state kinetic approach alone does not provide information about individual steps in the kinetic pathway. To probe the rate-determining steps in Csk, Cole, Walsh, and colleagues have applied viscosometric studies and concluded that phosphoryl transfer is partially rate-limiting in the presence of Mn^{2+} using polyGlu$_4$Tyr as a substrate (*6*). In this study, we elected to analyze the individual steps in the Csk-catalyzed reaction using pre-steady-state and transient-state kinetic experiments and a substrate peptide, $K_4E_2IYF_3$, derived from a random library screening (*33*). This substrate was selected over the general heteropolymer, polyGlu$_4$Tyr, since it is homogeneous and contains a single, easily quantifiable phosphorylation site for rigorous biophysical analyses. For these studies, we utilized a bacterially expressed form of Csk (*37*). Free Csk can be separated from GST−Csk and GST after thrombin cleavage using ion exchange chromatography (Figure 1A). Purified Csk elutes from a size exclusion column as a single peak, consistent with a monomeric, folded protein (Figure 1B).

Scheme 1

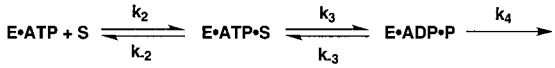

Phosphoryl Transfer Is Not Rate-Limiting in Csk. While prior viscosometric studies suggested that phosphoryl transfer is partially rate-limiting for turnover (*30*), we have shown in other studies that interpreting the effects of viscosogens on turnover is not always straightforward. For wild-type PKA, product release is only partially rate-limiting in k_{cat}, using physiological Mg^{2+} concentrations, yet a full viscosity effect is observed on this parameter (*17*, *19*). These results demonstrate that the effects of solvent additives on protein kinases must be interpreted carefully because of difficulties in assigning viscosity-sensitive and -insensitive steps. The application of rapid quench flow techniques, coupled with chemical detection methods, for the Csk reaction has the advantage of providing direct measurements on the phosphoryl transfer step. Using this approach, we showed that Csk phosphorylates a substrate peptide in a biphasic manner, in line with classic burst kinetics (Figure 2A). These data are consistent with the kinetic mechanism in Scheme 1 under conditions of high ATP concentrations, where substrate peptide binding is defined by the association and dissociation rate constants, k_2 and k_{-2}, respectively, the forward and reverse phosphoryl transfer steps are k_3 and k_{-3}, respectively, and the apparent release rate for products is k_4. A burst in the amount of phosphopeptide (P) is observed because the steps defined by k_2 and k_3 are fast relative to the k_4 step (*1*).

While the phosphoryl transfer step is not rate-limiting for substrate turnover, the available kinetic data do not permit an exact assignment of the k_3 step in Scheme 1. For the kinetic mechanism in Scheme 1, k_b can be expressed using eq 2 when the substrate peptide is in rapid exchange with the active site (*42*, *43*).[2]

$$k_b = \frac{k_3[S]}{[S] + K_d} + k_{-3} + k_4 \qquad (2)$$

For Csk, k_b increases linearly and shows no sign of reaching a maximum at the tested substrate peptide concentrations (Figure 3B). While this prohibits a direct measure of k_3,

[2] Two observations support a kinetic mechanism for Csk involving rapid equilibrium binding of substrate peptide (i.e., $k_{-2} > k_3$). First, there is no lag in the pre-steady-state kinetic burst phase at low substrate peptide concentrations (Figure 3A). Sigmoidal kinetics are expected if k_b/[S] (13 mM^{-1} s^{-1}) is limited by k_2 in Scheme 1 (*1*). Second, viscous media (25% sucrose) do not lower the value of k_{cat}/K_m, as expected if this term is limited by a simple bimolecular process, namely, k_2.

extrapolation of the plot to zero substrate peptide provides the sum $k_{-3} + k_4$ (25 s^{-1}). Later, it will be demonstrated that k_4 is low so that the intercept term reflects largely the value of k_{-3} (see the next section). The data in Figure 3B allow a lower limit to be placed on k_3. Since the K_m sets a lower limit on the K_d, we can use eq 2, the value of $k_{-3} + k_4$, and the highest value of k_b measured at 5 mM substrate peptide (Table 1) to place a lower limit of 140 s^{-1} on k_3. In fact, it is very likely that the K_d is much larger than K_m so that k_3 is even larger. Nonetheless, this estimate indicates that the phosphoryl transfer step is not rate-limiting in the Csk reaction. Also, a lower limit of 6 can be placed on the internal equilibrium constant ($K_{int} = k_3/k_{-3} \geq 140\ s^{-1}/25\ s^{-1}$) for the phosphoryl transfer reaction. This lower limit is consistent with independent measurements for protein kinases. For example, the internal equilibrium constant for PKA was found to be 100 using phosphorus NMR (*44*). While the internal equilibrium constant for the InRK is lower at a value of 10, it is still highly favorable (*11*).

Source of the Low Burst Amplitude. Previous studies have shown that phosphorylation of a substrate by PKA results in burst kinetics consistent with rapid phosphoryl transfer in the active site followed by slow turnover (*1*). In these experiments, the burst amplitude represents approximately 90−100% of the total protein concentration. In contrast, the amplitude of the burst phase for Csk is low compared to the enzyme concentration, reflecting approximately 6% of the total protein concentration at 5 mM substrate peptide (Table 1). There are three reasons why a low burst amplitude can be observed in a pre-steady-state kinetic experiment. First, the low amplitude could result from a large concentration of inactive or unproductive enzyme. While the data in Figure 1 indicate that Csk is a well-folded monomer (Figure 1), the enzyme could equilibrate between an active and inactive form which might not be readily resolved by ion exchange or size exclusion chromatography. Second, the burst amplitude will be attenuated if the phosphoryl transfer step is not favorable (i.e., $K_{int} \leq 1$) (see eq 3). We can dismiss this possibility because of the estimates placed on K_{int} from the data in Figure 3B. Third, the amplitude will be diminished under subsaturating concentrations of substrate.

For the mechanism in Scheme 1, the amplitude (α) can be expressed using eq 3 when the substrate is in rapid exchange ($k_{-2} > k_3$),[2] the apparent release rate for products is slow ($k_{-3} > k_4$),[3] and the apparent rate of k_3 is faster than k_4 [i.e., $k_3[S]/([S] + K_d) > k_4$] (*42*, *43*).

$$\frac{\alpha}{E_{tot}} = \left[\left(\frac{k_3}{k_3 + k_{-3}}\right)\left(\frac{[S]}{[S] + K_m}\right)\right]^2 \qquad (3)$$

Equation 3 predicts that α will be diminished at subsaturating substrate concentrations and/or when the internal equilibrium constant is unfavorable. Since we demonstrated that the latter does not apply, we will consider the effects of the substrate peptide concentration on the burst amplitude. On the basis of the K_m measurement, at 5 mM substrate peptide the expected value of α/E_{tot} is 0.25, a value 4-fold larger than the average α/E_{tot} (Figure 2B). Thus, it is likely that only 25% of the total protein is active. This value is similar to that reported for the receptor PTK, HER-2 (*12*). Given these observations, we conclude that the low, substoichiometric burst amplitudes observed in the rapid quench flow studies are not solely a result of high K_m values for the substrate. These findings imply that the current k_{cat} (0.12 s^{-1}) is underestimated by a factor 4 so that the true k_{cat}, corrected for inactive or unproductive enzyme, is approximately 0.5 s^{-1}. This number is much lower than the values for k_3 and k_{-3}, a finding that supports our previous assumptions [i.e., $k_{-3} > k_4$ and $k_3[S]/(K_d + [S]) > k_4$]. Since the phosphoryl transfer step is favorable ($K_{int} \geq 6$) and fast ($k_3 \geq 140\ s^{-1}$), the k_4 step limits turnover and has a value of approximately 0.5 s^{-1}.

What Is the Rate-Determining Step in Turnover? While the kinetic studies clearly demonstrate that the k_4 step is rate-limiting, they do not establish the physical nature of this step. Given the chemical means of evaluating substrate phosphorylation in these studies (i.e., isolation of phosphopeptide), k_4 could reflect rate-limiting release of one or both of the products or a slow conformational change. With regard to the former, there is no compelling evidence that release of the phosphoproduct limits turnover. The K_d for the substrate peptide is in excess of 5 mM so that its dissociation rate constant is likely to be large. Since a number of studies on protein kinases reveal that the phosphoproduct does not bind better than the substrate (*11*, *17*, *45*, *46*), the release rate for phosphopeptide is also likely to be much faster than the turnover rate. In contrast to the observed weak substrate peptide and phosphopeptide affinities, the K_m for ATP (20 μM) to Csk is comparatively low. In addition, Cole and colleagues have shown that the K_I for ADP is very low, 1.5 μM (*6*). Thus, nucleotide rather than phosphopeptide release is a more likely candidate for rate limitation in k_{cat}. We explored this possibility by measuring the dissociation rate constant for ADP using mant-ATP as a trapping agent. The fluorescent nucleotide displaces ADP at a rate constant of 0.6 s^{-1} (Figure 4), setting a maximum turnover rate for Csk. Since this dissociation rate is close to our estimated values for k_4 and k_{cat} (0.5 s^{-1}), we conclude that the rate-determining step in turnover is the release of ADP. Despite this correlation, it is likely that slow conformational changes play an important role in nucleotide binding and dissociation. Since doubling the solvent viscosity does not diminish proportionally k_{cat}, the release of ADP likely involves slow, structural steps. Consequently, the k_4 step in Scheme 1 comprises both product release and conformational change events, but it is the latter that exerts the greatest influence on setting the overall turnover rate for Csk. On the basis of trapping studies, Anderson and co-workers concluded that structural changes partially control product release in HER-2 (*12*). Given these studies and those for PKA (*17*, *19*) and Csk, the participation of slow conformational changes in turnover may be a general phenomenon for this enzyme family.

Substrate Processing in Csk. Through the application of pre-steady-state and transient-state kinetic studies, a kinetic mechanism for Csk can now be assembled. As shown in Figure 5, Csk rapidly phosphorylates the substrate peptide with a rate constant ($\geq$140 s^{-1}) that is more than 2 orders of magnitude greater than the turnover rate constant ($k_{cat} = 0.5$ s^{-1}). Consistent with prior measurements on the internal equilibrium for protein kinases (*11*, *44*), Csk favors substrate peptide phosphorylation over ADP phosphorylation by a

[3] Since the dissociation rate constant for ADP is 0.6 s^{-1} (Figure 4), the net value for k_4 is less than k_{-3} ($k_{-3} > k_4$).

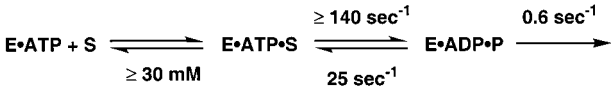

FIGURE 5: Kinetic mechanism of Csk derived from the pre-steady-state and transient-state kinetic experiments. The determination of the individual steps is outlined within the text.

factor of, at least, 6. While the dissociation rate constant for the phosphopeptide was not measured, it is presumed to be faster than the rate of turnover. Although we cannot make a direct measurement on substrate peptide affinity, we can place a lower limit of 30 mM on the K_d based on eq 2 and the slope of the data in Figure 3B. While the slow event in turnover is overall ADP release at 0.6 s^{-1}, this rate most likely reflects significant contributions from slow structural change steps because of the absence of a viscosity effect. The latter observation, in light of a fast rate of phosphoryl transfer, applies a restrictive note regarding the interpretation of viscosity effects on protein kinases. Namely, the absence of a viscosity effect does not imply that phosphoryl transfer is slow. The overall mechanism in Figure 5 bears similarities to that for PKA (*1*). While PKA represents a simple protein kinase, lacking contiguous regulatory domains, the rates of phosphoryl transfer in both enzymes are very similar (500 s^{-1} for PKA vs ≥ 140 s^{-1} for Csk). Thus, both enzymes have adapted to specifically phosphorylate unique side chains (serine for PKA and tyrosine for Csk) with excellent efficiency in the active site. Finally, both enzymes utilize slow conformational changes to assist in substrate processing. One of these conformational changes for both Csk and PKA occurs after the delivery of the γ-phosphate of ATP.

REFERENCES

1. Grant, B. D., and Adams, J. A. (1996) *Biochemistry **35***, 2022−9.
2. Robertson, S. C., Tynan, J., and Donoghue, D. J. (2000) *Trends Genet. 16*, 368.
3. Cohen, P. (1999) *Curr. Opin. Chem. Biol. 3*, 459−65.
4. Adams, J. A., McGlone, M. L., Gibson, R., and Taylor, S. S. (1995) *Biochemistry 34*, 2447−54.
5. Adams, J. A. (1996) *Biochemistry 35*, 10949−56.
6. Grace, M. R., Walsh, C. T., and Cole, P. A. (1997) *Biochemistry 36*, 1874−81.
7. Grant, B. D., Hemmer, W., Tsigelny, I., Adams, J. A., and Taylor, S. S. (1998) *Biochemistry 37*, 7708−15.
8. Saylor, P., Hanna, E., and Adams, J. A. (1998) *Biochemistry 37*, 17875−81.
9. Hirai, T. J., Tsigelny, I., and Adams, J. A. (2000) *Biochemistry 39*, 13276−84.
10. Konkol, L., Hirai, T. J., and Adams, J. A. (2000) *Biochemistry **39***, 255−62.
11. Ablooglu, A. J., and Kohanski, R. A. (2001) *Biochemistry 40*, 504−13.
12. Jan, A. Y., Johnson, E. F., Diamonti, A. J., Carraway, I. K., and Anderson, K. S. (2000) *Biochemistry 39*, 9786−803.
13. Hagopian, J. C., Kirtley, M. P., Stevenson, L. M., Gergis, R. M., Russo, A. A., Pavletich, N. P., Parsons, S. M., and Lew, J. (2001) *J. Biol. Chem. 276*, 275−80.
14. Zhou, J., and Adams, J. A. (1997) *Biochemistry 36*, 15733−8.
15. Aimes, R. T., Hemmer, W., and Taylor, S. S. (2000) *Biochemistry 39*, 8325−32.
16. Grant, B. D., Tsigelny, I., Adams, J. A., and Taylor, S. S. (1996) *Protein Sci. 5*, 1316−24.
17. Shaffer, J., and Adams, J. A. (1999) *Biochemistry 38*, 12072−9.
18. Andersen, M. D., Shaffer, J., Jennings, P. A., and Adams, J. A. (2001) *J. Biol. Chem. 276*, 14204−11.
19. Shaffer, J., and Adams, J. A. (1999) *Biochemistry 38*, 5572−81.
20. Zheng, J., Knighton, D. R., Ten Eyck, L. F., Karlsson, R., Xuong, N., Taylor, S. S., and Sowadski, J. M. (1993) *Biochemistry 32*, 2154−61.
21. Hunter, T. (1994) *Semin. Cell Biol. 5*, 367−76.
22. Okada, M., and Nakagawa, H. (1989) *J. Biol. Chem. 264*, 20886−93.
23. Sicheri, F., and Kuriyan, J. (1997) *Curr. Opin. Struct. Biol. 7*, 777−85.
24. Imamoto, A., and Soriano, P. (1993) *Cell 73*, 1117−24.
25. Thomas, S. M., Soriano, P., and Imamoto, A. (1995) *Nature 376*, 267−71.
26. Lamers, M. B., Antson, A. A., Hubbard, R. E., Scott, R. K., and Williams, D. H. (1999) *J. Mol. Biol. 285*, 713−25.
27. Sicheri, F., Moarefi, I., and Kuriyan, J. (1997) *Nature 385*, 602−9.
28. Williams, J. C., Weijland, A., Gonfloni, S., Thompson, A., Courtneidge, S. A., Superti-Furga, G., and Wierenga, R. K. (1997) *J. Mol. Biol. 274*, 757−75.
29. Xu, W., Harrison, S. C., and Eck, M. J. (1997) *Nature 385*, 595−602.
30. Cole, P. A., Burn, P., Takacs, B., and Walsh, C. T. (1994) *J. Biol. Chem. **269***, 30880−7.
31. Cole, P. A., Grace, M. R., Phillips, R. S., Burn, P., and Walsh, C. T. (1995) *J. Biol. Chem. 270*, 22105−8.
32. Sun, G., and Budde, R. J. (1997) *Biochemistry 36*, 2139−46.
33. Sondhi, D., Xu, W., Songyang, Z., Eck, M. J., and Cole, P. A. (1998) *Biochemistry 37*, 165−72.
34. Sondhi, D., and Cole, P. A. (1999) *Biochemistry 38*, 11147−55.
35. Sun, G., and Budde, R. J. (1999) *Biochemistry 38*, 5659−65.
36. Vang, T., Tasken, K., Skalhegg, B. S., Hansson, V., and Levy, F. O. (1998) *Biochim. Biophys. Acta 1384*, 285−93.
37. Sun, G., and Budde, R. J. (1995) *Anal. Biochem. 231*, 458−60.
38. Smith, D. B., and Johnson, K. S. (1988) *Gene 67*, 31−40.
39. Guan, K. L., and Dixon, J. E. (1991) *Anal. Biochem. 192*, 262−7.
40. Ni, Q., Shaffer, J., and Adams, J. A. (2000) *Protein Sci. 9*, 1818−27.
41. Martell, A. E., and Smith, R. M. (1977) *Critical Stability Constants*, Vol. 3, Plenum, New York.
42. Gutfreund, H. (1995) in *Kinetics for the life sciences: receptors, transmitters and catalysts*, Cambridge University Press, Cambridge, U.K.
43. Barman, T. E., and Travers, F. (1985) *Methods Biochem. Anal. 31*, 1−59.
44. Qamar, R., Yoon, M. Y., and Cook, P. F. (1992) *Biochemistry 31*, 9986−92.
45. Boerner, R. J., Barker, S. C., and Knight, W. B. (1995) *Biochemistry 34*, 16419−23.
46. Kwiatkowski, A. P., Huang, C. Y., and King, M. M. (1990) *Biochemistry 29*, 153−9.

BI011029Y